1632 © *1982 The Chemical Society of Japan* *Bull. Chem. Soc. Jpn.*, ***55***, *1632—1636 (1982)* [Vol. 55, No. 5

Electron Spin Resonance Studies of Manganese(II) Doped in $Cd(NH_3)_2Ni(CN)_4 \cdot 2C_6H_6$. Angular and Temperature Dependency of Fine Structures

Taku NAKANO

Department of Pharmaceutical Sciences, Toyama Medical and Pharmaceutical University, Toyama 930-01

(Received April 30, 1981)

ESR measurements on Mn(II) ion doped in single crystals of $Cd(NH_3)_2Ni(CN)_4 \cdot 2C_6H_6$ confirmed the structure of the Hofmann-type clathrate predicted before. Spin Hamiltonian parameters obtained are $g=2.0033 \pm 0.0010$, $A=(-84.9 \pm 1.0) \times 10^{-4}\ \mathrm{cm}^{-1}$ (123 K) and $(-84.3 \pm 1.0) \times 10^{-4}\ \mathrm{cm}^{-1}$ (room temp), $D=(67.5 \pm 1.0) \times 10^{-4}\ \mathrm{cm}^{-1}$ (123 K) and $(17.3 \pm 1.0) \times 10^{-4}\ \mathrm{cm}^{-1}$ (room temp), and $a=(16.5 \pm 1.0) \times 10^{-4}\ \mathrm{cm}^{-1}$. The environment of Mn(II) ion has a tetragonally distorted cubic symmetry. While the parameter a is independent of temperature, the parameter D is found to be dependent on temperature obeying to $D \propto (T_0-T)^2$ where T_0 is 473 K. The nuclear forbidden lines, $\Delta m = \pm 1$, were also detected, intensities of which vary in terms of D squared.

The series of Hofmann-type clathrates has the general formula of $M(NH_3)_2M'(CN)_4 \cdot 2G$, (M–M′–G), where M is a divalent metal ion such as Mn(II), Fe(II), Co(II), Ni(II), Cu(II), Zn(II), and Cd(II), and M′ is Ni(II), Pd(II), or Pt(II).[1–3] G represents an aromatic molecule such as benzene (Bz), aniline *etc.* The inorganic part of the compound, $M(NH_3)_2M'(CN)_4$, forms a two-dimensional network which clathrate aromatic molecules between them as shown in Fig. 1.[4–6]

X-Ray crystallographic investigations have been reported in cases of Mn–Ni–Bz,[6] Ni–Ni–Bz,[4] Cu–Ni–Bz,[7] and Cd–Ni–Bz.[5] The compounds have an isomorphous structure with a space group of P4/m.

Magnetic properties of the clathrates have been reported for Mn–Ni–G,[8] Ni–Ni–G,[9] and Cu–Ni–G.[10] The ^{1}H NMR of ammonia molecules, which coordinate to metal ion M, is also reported in both diamagnetic[11] and paramagnetic[12,13] compounds. ESR study of copper(II) has shown the Jahn-Teller distortion around the copper(II) ion which reveals that d_{z^2} orbital is the ground state.[7,14,15]

The manganese(II) ion in Hofmann-type clathrate has a high spin d^5 structure and the orbital angular momentum is quenched. The purpose of this study is to clarify the behavior of the paramagnetic manganese(II) ion which will reflect the fundamental characters of Hofmann-type clathrates by means of ESR spectroscopy.

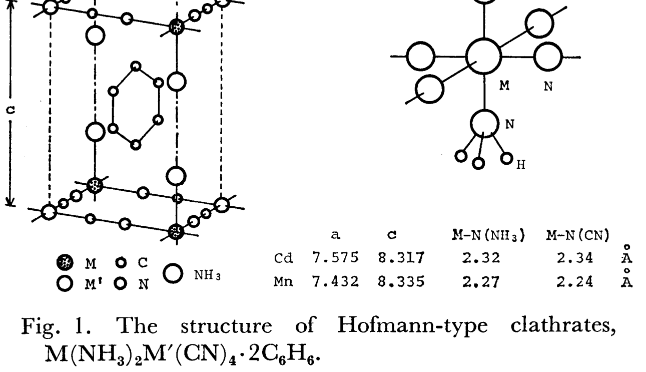

	a	c	M-N(NH3)	M-N(CN)	
Cd	7.575	8.317	2.32	2.34	Å
Mn	7.432	8.335	2.27	2.24	Å

Fig. 1. The structure of Hofmann-type clathrates, $M(NH_3)_2M'(CN)_4 \cdot 2C_6H_6$.

Experimental

The single crystals of Cd–Ni–Bz which contain 0.1% of manganese(II) were prepared from an aqueous layer of an ammoniacal solution containing 1×10^{-2} mol dm^{-3} $Cd(NO_3)_2$, 1×10^{-5} mol dm^{-3} $MnCl_2$, 1×10^{-2} mol dm^{-3} $K_2Ni(CN)_4$, and 0.5 mol dm^{-3} NH_4Cl: pH adjusted to 8—9 using ammonia, and an organic layer of toluene containing benzene. The crystals grew at the interface between the aqueous and organic layers and on the bottom of the vessel. The dimension of the single crystal investigated in the present study is *ca.* $0.5 \times 0.5 \times 1.0$ mm^3 of the form of a square pillar, having ends in the form of pyramids.

The preparation of the crystals and the measurements of the ESR were done under a nitrogen atmosphere to prevent manganese(II) ions from being oxidized.

The ESR spectra were recorded using JES-FE-3X spectrometer at an X band frequency: 9.2 GHz, and a field modulation of 100 KHz and modulation widths of 0.4 mT. The field was calibrated with signals of manganese(II) doped in MgO. The crystal was rotated about the [001] and [110] axes and the temperature was varied with a stream of cold nitrogen, measured by a copper-constantan thermocouple.

Results and Discussion

The ESR spectra were recorded at various temperatures and at various angles, θ and φ; θ is the angle between the field and the [001] axis of the crystal and φ is that between the field in the (001) plane and [110] axis.

Figure 2 shows the ESR spectra recorded at various angles, θ, at 123 K. The spectral change when the magnetic field rotated about [001] axis at 123 K reveals the fourfold symmetry, on the other hand that about [110] axis reveals the twofold symmetry. The symmetry indicated above confirms the structure of the Hofmann-type clathrates.

It is reasonable to assume that the manganese(II) ions are located at the same positions as the cadmium(II) ions in Cd–Ni–Bz crystals. The X-ray crystallographic investigations have shown that the environment of manganese(II) in Mn–Ni–Bz[6] as well as that of cadmium(II) in Cd–Ni–Bz[5] has D_{4h} symmetry. The detailed structural parameters, the lattice con-

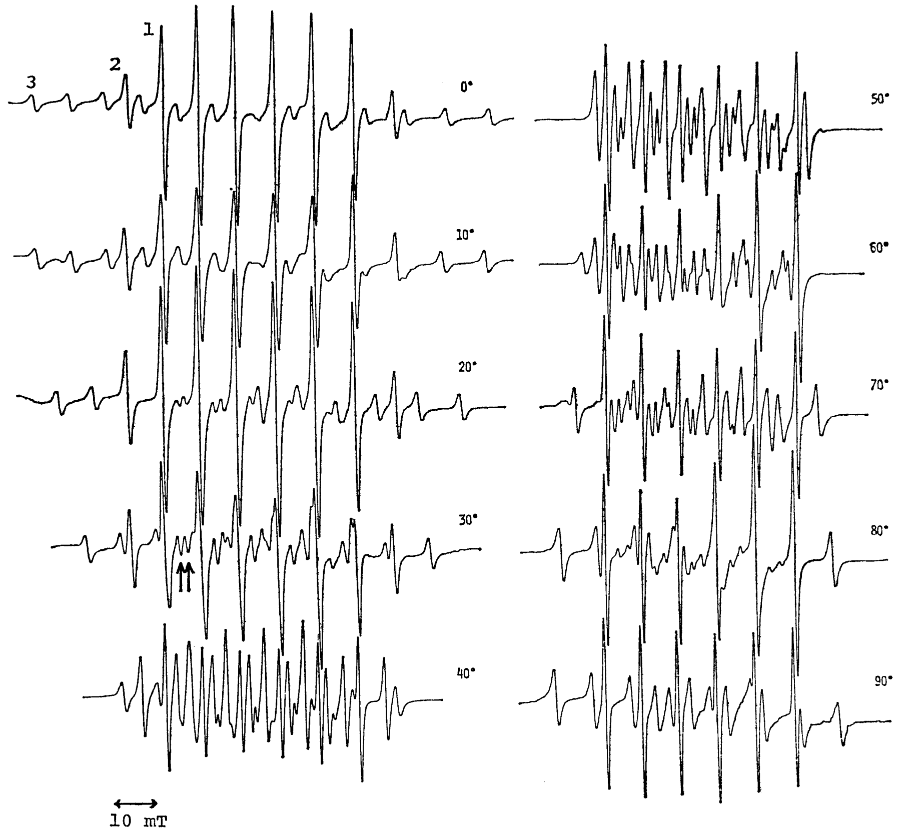

Fig. 2. ESR spectral change on angle θ at 123 K and $\varphi=0°$.
1: $|M,m\rangle = |1/2,5/2\rangle \leftrightarrow |-1/2,5/2\rangle$, 2: $|M,m\rangle = |1/2,5/2\rangle \leftrightarrow |3/2,5/2\rangle$, 3: $|M,m\rangle = |3/2,5/2\rangle \leftrightarrow |5/2,5/2\rangle$. Arrows in the spectrum at $\theta=30°$ indicate the nuclear forbidden transitions: see text.

stants and the metal-nitrogen distances, are quoted in Fig. 1 to compare both compounds.[5,6)]

The comparison of the metal-nitrogen distances has permitted us to assume the conservation of symmetry D_{4h} about manganese(II) ions doped in Cd-Ni-Bz. Thus the magnanese(II) ion was treated as having a nearly cubic but slightly tetragonally distorted structure of a weak crystalline field, and the assumption was revealed to be good.

The explanation of the spectra and the spectral changes can be made with a spin Hamiltonian of the form:

$$\begin{aligned}\mathscr{H} &= \beta \boldsymbol{H}\cdot\boldsymbol{g}\cdot\boldsymbol{S} + D[S_z^2 - S(S+1)/3] + E(S_x^2 - S_y^2) \\ &\quad + \frac{1}{6}a\left[S_x^4 + S_y^4 + S_z^4 - \frac{1}{5}S(S+1)(3S^2+3S-1)\right] \\ &\quad + \boldsymbol{S}\cdot\boldsymbol{A}\cdot\boldsymbol{I} - g_n\beta_n\boldsymbol{H}\cdot\boldsymbol{I}, \qquad (1)\end{aligned}$$

where D and E are axial and rhombic distortion parameters, respectively. The quantity a is a cubic parameter of the fourth order. Other symbols have their ordinary meanings.

The fields of the allowed transitions that are used for a high spin d^5 system of manganese(II) assuming the spin Hamiltonian (1) are calculated by the following equations:[16)] it is also assumed that g and A are isotropic according to the results shown later.

$$\begin{aligned}M = \left|\pm\frac{5}{2}\right\rangle \leftrightarrow \left|\pm\frac{3}{2}\right\rangle:\ H &= H_0 \mp 2\left(\frac{D}{g\beta}\right)(3\cos^2\theta - 1) \\ &\quad - \frac{32}{H_0}\left(\frac{D}{g\beta}\right)^2 \cos^2\theta \sin^2\theta \\ &\quad + \frac{1}{H_0}\left(\frac{D}{g\beta}\right)^2 \sin^4\theta \mp 2p\left(\frac{a}{g\beta}\right) + f(M,m), \\ M = \left|\pm\frac{3}{2}\right\rangle \leftrightarrow \left|\pm\frac{1}{2}\right\rangle:\ H &= H_0 \mp \left(\frac{D}{g\beta}\right)(3\cos^2\theta - 1) \\ &\quad + \frac{4}{H_0}\left(\frac{D}{g\beta}\right)^2 \cos^2\theta \sin^2\theta \\ &\quad - \frac{5}{4H_0}\left(\frac{D}{g\beta}\right)^2 \sin^4\theta \pm \frac{5}{2}p\left(\frac{a}{g\beta}\right) + f(M,m), \\ M = \left|+\frac{1}{2}\right\rangle \leftrightarrow \left|-\frac{1}{2}\right\rangle:\ H &= H_0 + \frac{16}{H_0}\left(\frac{D}{g\beta}\right)^2 \cos^2\theta \sin^2\theta \\ &\quad - \frac{2}{H_0}\left(\frac{D}{g\beta}\right)^2 \sin^4\theta + f(M,m), \qquad (2)\end{aligned}$$

where M and m mean electron and nuclear(^{55}Mn) magnetic quantum numbers respectively, and $p=1-5(l^2m^2+m^2n^2+n^2l^2)$ and l, m, and n are direction cosines of the magnetic field with respect to the x, y, and z axes, respectively. The last terms correspond to a hyperfine splitting for the transition $|M\rangle \leftrightarrow |M-1\rangle$, $\Delta m=0$, to be expressed as;

$$f(M,m) = -\left(\frac{A}{g\beta}\right)m - \frac{1}{2H_0}\left(\frac{A}{g\beta}\right)^2 \times \left[\frac{35}{4} - m^2 + m(2M-1)\right]. \qquad (3)$$

Table 1. Spin Hamiltonian parameters

	Parameters	T/K
$g(g_{//}=g_{\perp})$	2.0033 ± 0.0010	
$A(A_{//}=A_{\perp})/\mathrm{cm}^{-1}$	$(-84.9\pm1.0)\times10^{-4}$	123
	$(-84.3\pm1.0)\times10^{-4}$	room
D/cm^{-1}	$(67.5\pm1.0)\times10^{-4}$	123
	$(17.3\pm1.0)\times10^{-4}$	room
E/cm^{-1}	0	
a/cm^{-1}	$(16.5\pm1.0)\times10^{-4}$	

In Fig. 2, the most intense sextet is assigned to be $|-1/2\rangle\leftrightarrow|1/2\rangle$ transition, the middle ones are $|\pm1/2\rangle\leftrightarrow|\pm3/2\rangle$ transitions and the weakest are $|\pm3/2\rangle\leftrightarrow|\pm5/2\rangle$ transitions.

The Hamiltonian parameters were obtained from the spectra both at room temperature and at 123 K and are listed in Table 1. The shifts of signal positions *versus* angle θ arise from D and a terms and those *versus* φ only from a term. The g value and the hyperfine constant A are isotropic namely $g=g_{//}=g_{\perp}$ and $A=A_{//}=A_{\perp}$ within the experimental error.

The absolute signs of the parameters were determined by considering the angular dependency of the signal positions according to Eqs. 2 and 3, where the second order approximation was dealt with. If $D\cdot A<0$, for the sextet of the transition of $M>0$, the splitting caused by Eq. 3 is smaller, and the position at $\theta=0°$ is at a lower field than that of $M<0$ or *vice versa*. This is the case. The change of the signal positions on angle θ make it clear that the parameters D and a have the same sign. When A is assumed to be negative, as general, the sign of a is positive being consistent with Watanabe's theory.[17] The signs of the parameters thus obtained are shown in Table 1. Other sets of signs do not explain the change of the signal positions.

The thirty angular dependence curves calculated according to Eq. 2 using the parameter values in Table 1 are in a good agreement with the experimental results shown in Figs. 3 and 4, where the assignments are indicated.

Temperature Dependency of the Fine Structures. As reported in many cases of manganese(II) ESR, the parameter D has non-zero values also in the Hofmann-type clathrate, though g and A are isotropic. Here, it is noteworthy that the D value is dependent on temperature. The changes of the signal positions due to temperature are shown in Fig. 5 in the temperature region from 123 to 433 K. Above room temperature the signals were irreversibly broadened because of an escape of benzene molecules from the surface of the crystal.

While the signal positions of the sextet $M=|1/2\rangle\leftrightarrow|-1/2\rangle$ do not vary with temperature, those of the sextets $M=|\pm1/2\rangle\leftrightarrow|\pm3/2\rangle$ and $M=|\pm3/2\rangle\leftrightarrow|\pm5/2\rangle$ shift outwards with decreasing temperature. The values of the parameters D and a are plotted in Fig. 6.

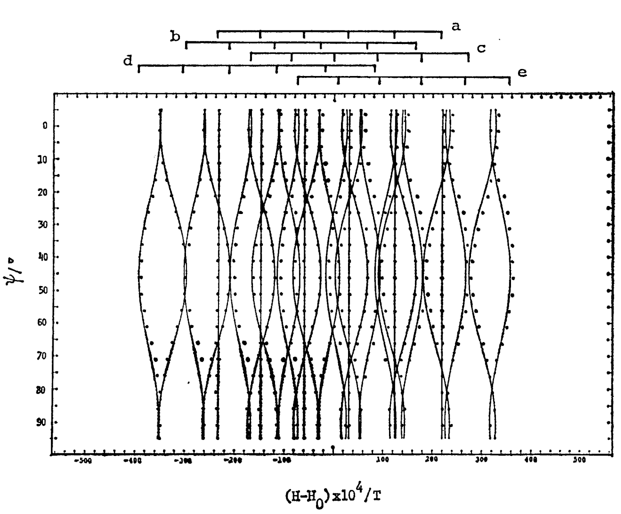

Fig. 3. Angular dependence of ESR signals on angle φ at $\theta=90°$.
$H_0=3274\times10^{-4}$ T. Dots are the experimental results and the solid lines are calculated curves using the parameter values at 123 K in Table 1. The signal positions are assigned at $\varphi=45°$. a: $|M\rangle=|1/2\rangle\leftrightarrow|-1/2\rangle$, b: $|M\rangle=|-1/2\rangle\leftrightarrow|-3/2\rangle$, c: $|M\rangle=|1/2\rangle\leftrightarrow|3/2\rangle$, d: $|M\rangle=|-3/2\rangle\leftrightarrow|-5/2\rangle$, e: $|M\rangle=|3/2\rangle\leftrightarrow|5/2\rangle$. As for m, the lowest is assigned to be $m=-5/2$ and the highest 5/2 for all five sextets.

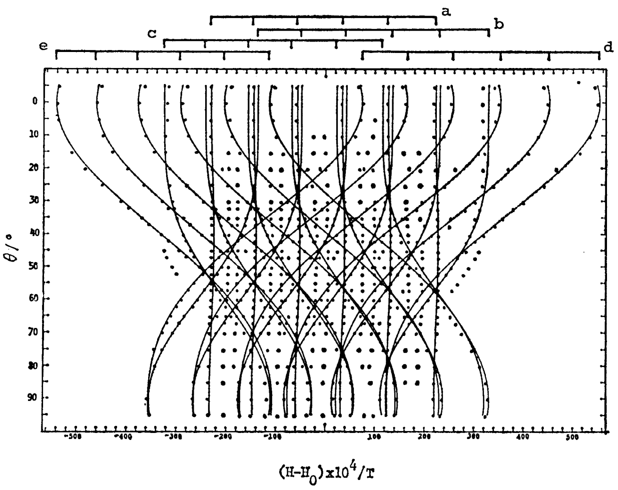

Fig. 4. Angular dependence of ESR signals on angle θ at $\varphi=0°$.
$H_0=3274\times10^{-4}$ T. Dots are the experimental results and the solid lines are calculated curves using the parameter values at 123 K in Table 1. The signal positions are assigned at $\theta=0°$. a: $|M\rangle=|1/2\rangle\leftrightarrow|-1/2\rangle$, b: $|M\rangle=|-1/2\rangle\leftrightarrow|-3/2\rangle$, c: $|M\rangle=|1/2\rangle\leftrightarrow|3/2\rangle$, d: $|M\rangle=|-3/2\rangle\leftrightarrow|-5/2\rangle$, e: $|M\rangle=|3/2\rangle\leftrightarrow|5/2\rangle$. As for m, the lowest is assigned to be $m=-5/2$ and the highest 5/2 for all five sextets.

As shown clearly in Fig. 6, the cubic parameter a is independent of temperature. Since the parameter a relates closely with the strength of the cubic crystalline field parameter Dq, as indicated by Watanabe,[17] the constancy of the parameter a suggests that the crystalline field does not vary as the results of the structural change around manganese(II) ions in the temperature region studied here.

According to Watanabe,[17] the crystalline field parameter Dq is estimated to be $1407\ cm^{-1}$. Unfortunately the spectroscopic data was not available for comparison with the theoretical value in this stage.

On the other hand, the parameter D increases with decreasing temperature as shown in Figs. 6 and 7. In Fig. 7 the square root of D is plotted and has a linear relation to temperature. Thus the temperature dependency of D was found experimentally to be

$$D(T) = k(T_0 - T)^2, \tag{4}$$

where T is the absolute temperature and T_0 and k were found to be 473 K and $5.2_7\times10^{-8}\ cm^{-1}\ K^{-2}$ respectively.

The temperature dependence of D has been found for example in cases of nickel(II) ESR in $NiSnCl_6\cdot 6H_2O$,[18] and $NiSiF_6\cdot 6H_2O$,[19] manganese(II) ESR in K_2SO_4,[20] and iron(III) ESR in $BaTiO_3$;[21] in the latter two cases the changes of D are attended on phase transitions. However the clear elucidation of these phenomena has not been given until now. In the case of manganese(II) in the Hofmann-type clathrate, any structural change has not been reported in the temperature region studied here and moreover the invariability of the parameter a does not suggest any phase transitions. Though the reason for the temperature dependency cannot be elucidated in this stage, this phenomenum would add a new characteristic feature on the Hofmann-type clathrates. Further investigation of the structure will be necessary.

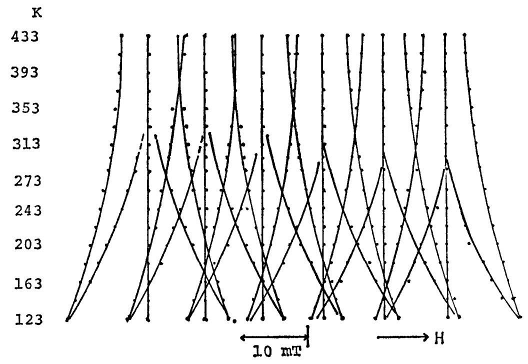

Fig. 5. Temperature dependence of the ESR signals at $\theta=90°$ and $\varphi=0°$.

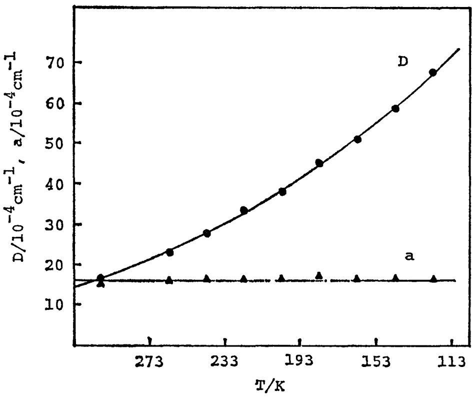

Fig. 6. Relations between D and a parameters and temperature.

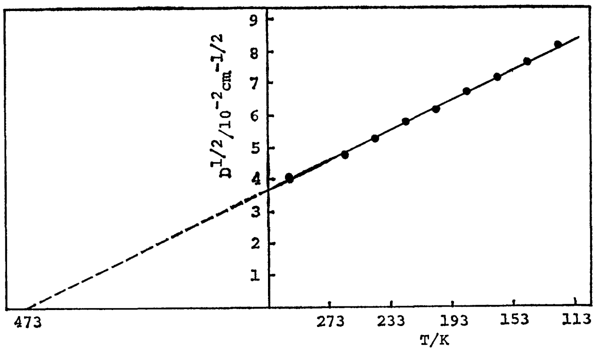

Fig. 7. Temperature dependence of D parameter.

The Nuclear Forbidden Lines. The arrows in the spectra in Figs. 2 and 8 indicate the nuclear forbidden lines, $\Delta m=\pm1$. The intensities of these lines found here do change with temperature. The number of theoretically predicted forbidden lines is thirty, but in this case we could find the relatively intense five doublets that appear among the sextet of allowed transitions $|1/2\rangle\leftrightarrow|-1/2\rangle$, and others that are barely recognizable outside the intensive allowed signals near $\theta=50°$. In Fig. 4, the dots aside from the solid lines mark the positions of the forbidden lines. The forbidden lines appear when the magnetic field

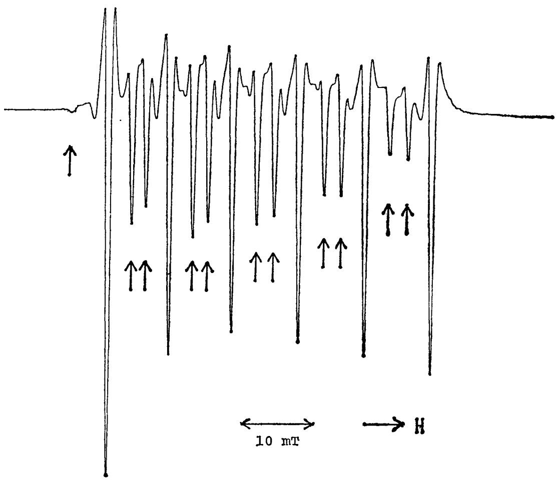

Fig. 8. Nuclear forbidden lines at $\theta=55°$ and $\varphi=0°$, and at 113 K. The spectrum is a second derivative curve. Five doublets are assigned to be $M=|1/2\rangle-|-1/2\rangle$, $\Delta m=\pm1$, and the arrow at the lowest field indicates the one not assigned.

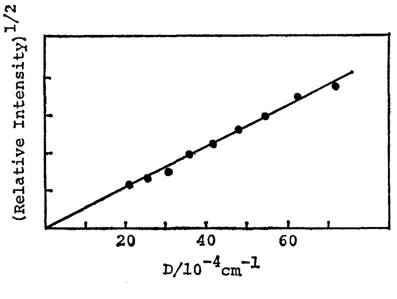

Fig. 9. Relation between D and intensity of the forbidden lines: $\Delta M=\pm1$ and $\Delta m=\pm1$.

is rotated about the [110] axis, disappearing at $\theta=0°$ and 90°, and not observed when the field is rotated about the [001] axis. The signals have maximum intensities near $\theta=55°$. Unfortunately the precise determination of the change of intensity with rotation was impossible since the strong signals of the allowed transitions superimpose on the forbidden lines.

The relative intensity increases with decreasing temperature, suggesting that it is related closely with the D value. Figure 9 shows the relation between the intensity of one of the pairs of the doublets and the axial parameter D at $\theta=55°$, at which angle the forbidden lines clearly appear separated from the allowed transitions. The intensity is proportional to D^2;

$$I(1/2) = k(\theta)D^2, \qquad (5)$$

where $I(1/2)$ is the intensity of the forbidden line $M=|1/2\rangle \leftrightarrow |-1/2\rangle$, and $k(\theta)$ is a function of angle θ.

The intensity of the forbidden lines will vary as $\mathrm{A}\cdot D^2(\sin 2\theta)^2+\mathrm{B}\cdot a^2(\sin 4\theta)^2$, when the parameters D and a have non-zero values.[22,23] However the relation revealed in this compound between the intensity and the parameter D suggests that the mixing of the energy states may arise from the second order perturbation only with the D term, and those with the a term would be too small to be detected here.

The positions of the forbidden lines $M=|1/2\rangle \leftrightarrow |-1/2\rangle$ and the separations of the doublets were independent of temperature. The separations of doublets obtained experimentally are $18._7$, $20._6$, $23._4$, $23._4$, and $25._3\times10^{-4}\,\mathrm{cm}^{-1}$ for $m=|-5/2\rangle \leftrightarrow |-3/2\rangle$, $m=|-3/2\rangle \leftrightarrow |-1/2\rangle$, $m=|-1/2\rangle \leftrightarrow |+1/2\rangle$, $m=|1/2\rangle \leftrightarrow |3/2\rangle$, and $m=|3/2\rangle \leftrightarrow |5/2\rangle$, respectively. The calculated values according to Bleaney and Rubins[22] are $18._8$, $20._7$, $22._3$, $23._9$, and $25._8\times10^{-4}\,\mathrm{cm}^{-1}$, respectively. The detailed work about the seperation will give the precise values of g_n and Q (quadrapole moment) of ^{55}Mn.

Conclusion

From the parameter values obtained, manganese(II) ion has a g value which is almost the same as that of a free electron, and slightly tetragonally distorted cubic symmetry, $\mathrm{D_{4h}}$. It is noteworthy that the axial parameter D is dependent on the temperature. This suggests a new characteristic feature in this compound, while the cubic parameter a does not change. The forbidden transitions arise from the D term and are also dependent on temperature.

The work was supported by a Grant-in-Aid for Scientific Research No. 474265 from the Ministry of Education, Science and Culture.

References

1) T. Nakano, T. Miyoshi, T. Iwamoto, and Y. Sasaki, *Bull. Chem. Soc. Jpn.*, **40** 1297 (1967).

2) M. Morita, T. Miyoshi, T. Iwamoto, T. Miyamoto, and Y. Sasaki, *Bull. Chem. Soc. Jpn.*, **40** 1556 (1967).

3) T. Iwamoto, T. Nakano, M. Morita, T. Miyoshi, T. Miyamoto, and Y. Sasaki, *Inorg. Chim. Acta*, **2**, 313 (1968).

4) J. H. Rayner and H. M. Powell, *J. Chem. Soc.*, **1959**, 319.

5) Y. Sasaki, *Bull. Chem. Soc. Jpn.*, **42**, 2412 (1969).

6) R. Kuroda and Y. Sasaki, *Acta Crystallogr.*, *Sect. B*, **30**, 687 (1974).

7) T. Miyoshi, T. Iwamoto, and Y. Sasaki, *Inorg. Chim. Acta*, **7**, 97 (1973).

8) H. Kitaguchi, S. Nagata, and T. Watanabe, *J. Phys. Soc. Jpn.*, **41**, 1159 (1976).

9) S. Takayanagi and T. Watanabe, *J. Phys. Soc. Jpn.*, **28**, 296 (1970).

10) H. Kitaguchi, S. Nagata, and T. Watanabe, *J. Phys. Soc. Jpn.*, **38**, 998 (1975).

11) T. Miyamoto, *Inorg. Chim. Acta*, **3**, 511 (1969).

12) T. Nakano, *Bull. Chem. Soc. Jpn.*, **46**, 2124 (1973).

13) S. Takayanagi and T. Watanabe, *J. Phys. Soc. Jpn.*, **31**, 109 (1971).

14) R. Murugesan and S. Subramanian, *J. Magn. Reson.*, **36**, 389 (1979).

15) S. Nagata, Y. Miyako, and T. Watanabe, *J. Phys. Soc. Jpn.*, **34**, 1158 (1973).

16) B. Bleaney and D. J. E. Ingram, *Proc. R. Soc. London, Ser. A*, **205**, 336 (1951).

17) H. Watanabe, *Prog. Theor. Phys.*, **18**, 405 (1957).

18) Y. Ajiro, S. A. Friedberg, and N. S. VanderVen, *Phys. Rev. B*, **12**, 39 (1975).

19) R. P. Penrose and K. W. H. Stevens, *Proc. Phys. Soc. London*, **A63**, 29 (1950).

20) B. V. R. Chowdari and P. Venkateswarlu, *J. Chem. Phys.*, **48**, 318 (1968).

21) A. W. Hornig, R. C. Rempel, and H. E. Weaver, *J. Phys. Chem. Solids*, **10**, 1 (1959).

22) B. Bleaney and R. S. Rubins, *Proc. Phys. Soc. London*, **77**, 103 (1961).

23) J. E. Drumheller and R. S. Rubins, *Phys. Rev. A*, **133**, 1099 (1964).